Analytical Method for Generalization of Numerically Optimized Inductor Winding Shapes

Jiankun Hu
C. R. Sullivan

Found in *IEEE Power Electronics Specialists Conference,* June 1999, pp. 568–573.

©1999 IEEE. Personal use of this material is permitted. However, permission to reprint or republish this material for advertising or promotional purposes or for creating new collective works for resale or redistribution to servers or lists, or to reuse any copyrighted component of this work in other works must be obtained from the IEEE.

Analytical Method for Generalization of Numerically Optimized Inductor Winding Shapes

Jiankun Hu* Charles R. Sullivan
Thayer School of Engineering
Dartmouth College, Hanover, NH 03755-8000
chrs@dartmouth.edu, http://thayer.dartmouth.edu/inductor

Abstract—A method is developed to use a single set of two-dimensional numerical optimizations of inductor winding shapes to simply calculate the optimal winding configuration for any design on the same core without repeating the computationally intensive numerical optimization. For transformer windings, the results are consistent with previous one-dimensional optimizations, but for inductor windings, analysis of two-dimensional effects allows significant performance improvements.

I. Introduction

In an inductor winding, the core, and particularly the air gap, strongly affect the field in the winding area, and thus determine proximity-effect losses in the winding. Conventional one-dimensional analyses of proximity-effect losses and the associated design methodologies developed for transformers [1-10] do not account for the true field of a gapped inductor, and do not allow accurate prediction of inductor ac resistance [11]. High-frequency winding losses are particularly important in applications with high ac currents, such discontinuous-mode converters, popular for high-power-factor converters, and resonant soft-switching converters. Low ac resistance is essential for efficient operation and thermal management.

In [12], numerical computation and optimization methods accounting for two-dimensional field effects were developed, and the resulting winding shapes were shown to provide significant reductions in losses, allowing the performance of a lumped-gap inductor to not only equal, but surpass the performance of a distributed-gap [13, 14] design. Thus, higher performance is achieved while avoiding the high cost of special low-permeability distributed-gap materials, or of complex quasi-distributed-gap construction [15-21].

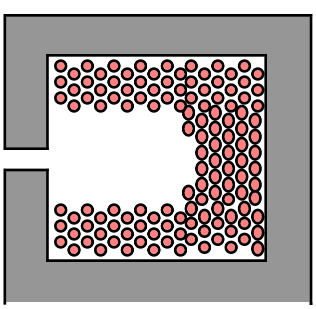

Fig. 1. Two-dimensional inductor with optimized winding shape.

* Now with Lucent Technologies

The method in [12] requires a numerical optimization for each design variation. In this paper, we show that, for a particular core shape, complete information may be obtained with a limited set of optimizations. This information may then be used to develop an analytical solution for minimum-loss winding designs for any inductor built on the same core. This makes it simple to design a low-loss inductor on a given core shape, for any set of electrical requirements. It is also is an important step toward optimizing core designs to take advantage of the possibilities afforded by optimized winding shapes.

II. Numerically Computed Optimum Winding Shapes

Our objective is to find optimized winding shapes for a fixed core and gap geometry and a fixed number of turns. In

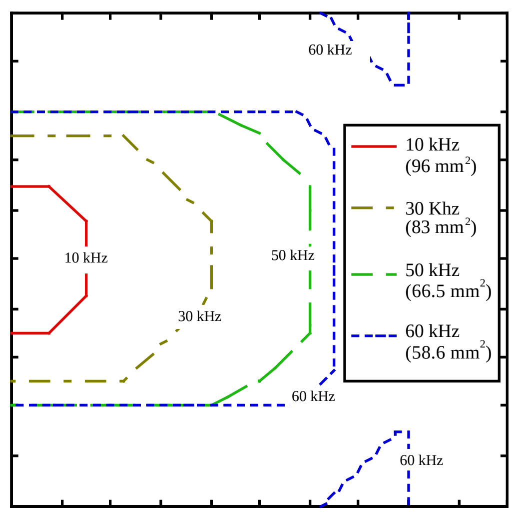

Fig. 2. Optimal winding shapes computed for a 10 mm x 10 mm winding window with a gap at the center left and 0.1 mm litz-wire strand diameter, for four frequencies. The area near the gap, bordered by the appropriate line for a given frequency, is empty of conductors. Cross-sectional area used by each solution is indicated. For the 60 kHz (58.6 mm^2) solution, additional empty areas appear at the top and bottom right.

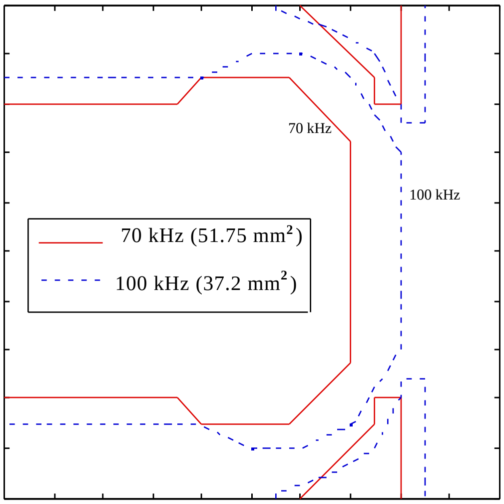

Fig. 3. Optimal winding shapes as in Fig. 2, but for higher frequencies. Areas empty of wire are bordered by the lines shown and include a "mushroom" shape based at the gap, bordered by the indicated line, and the wedges at the top and bottom right.

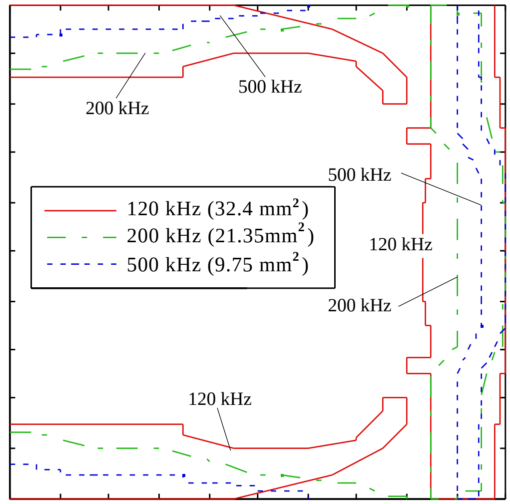

Fig. 4. Optimal winding shapes as in Figs. 2 and 3, but for higher frequencies. Conductors fill the indicated areas along the top and bottom walls and near the right wall.

[12], the use of litz wire is addressed, and a fixed strand diameter is assumed. The optimization problem is the choice of the number of strands in the litz bundle (assumed equal for each turn), and the positioning of the resulting bundles within the window. This means finding a region of the winding window, with area equal to the area of the wire (adjusted by a packing factor) that gives minimum total loss. The considerations involve include the tradeoff between lower ac loss with less copper and lower dc resistance with more copper; the positioning of the wire in regions of low field to minimize proximity-effect loss; and the effect of that position, in turn, on the field in the window area.

A sketch of the type of design that results from the optimization in [12] is shown in Fig. 1. Detailed results for an example design (a square winding window, 10 mm x 10 mm, and 0.1 mm strand diameter) are shown in Figs. 2, 3 and 4.

III. Generalized Analysis of Results

We would like to be able to apply the results of this numerical optimization to any winding design on the same core, even though the number of turns, the choice of whether to use litz or single-strand wire, the frequency and waveform of the current, and the strand diameter (if litz wire is to be used) may be different from those assumed in the original numerical optimization.

For cylindrical conductors with diameter, d, small compared to a skin depth, the proximity-effect loss in a sinusoidal ac field of amplitude B, perpendicular to the axis of the wire, at a frequency ω is [22],

$$P_{pe} = \frac{\pi \cdot \omega \cdot |\mathbf{B}|^2 \cdot l \cdot d^4}{128 \cdot \rho_c}, \qquad (1)$$

where l is the length of the conductor and ρ_c is the resistivity of the conductor. For nonsinusoidal flux waveforms, resulting from nonsinusoidal currents, (1) and the analysis below apply directly if an effective frequency, ω_{eff} [23], is substituted for ω. Calculation of the effective frequency is explained in the Appendix.

For the complete winding,

$$P_{pe} = \frac{\pi\omega^2 F_p}{128\rho_c} l d^2 \int_{A_1} |B|^2 \cdot dA \qquad (2)$$

where A_1 is the portion of the window that is actually used and F_p is the winding packing factor for that region. The proximity effect loss is proportional to the area times the average value of the square of the flux density, $A_1 \overline{|B|^2}$. The dc loss, however, is inversely proportional to A_1.

$$P_{dc} = \frac{4 I_{total}^2 \rho_c l}{\pi \cdot F_p A_1} \qquad (3)$$

Thus, the relationship between A_1 and $\overline{|B|^2}$ determines the proximity effect vs. dc loss tradeoff. This relationship depends only on the core geometry and winding shape, and not on the particulars of winding design, if we normalize $\overline{|B|^2}$ to the total winding current $NI = I_{total}$. We define this normalized function as

$$g(A_1) = \frac{\overline{|B|^2}}{I_{total}^2}. \qquad (4)$$

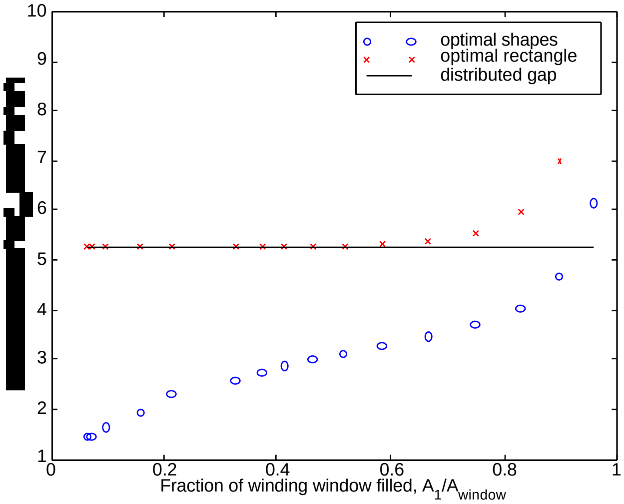

Fig. 5. Normalized average square of magnetic field, $g(A) = \overline{|B|^2}/I^2$, as a function of winding area for configurations based on three different design approaches. The solid line represents a rectangular winding with a distributed gap. The 'x's are for designs using a rectangular winding and a lumped gap, with the winding spaced as far from the gap as possible. The circles represent the optimal designs computed numerically.

This function may be found from one set of numerical optimization data, such as that shown in Fig. 2-4, and is shown in Fig. 5. We will show that this data can then be used to derive expressions for the optimum winding configuration given several different possible sets of constraints.

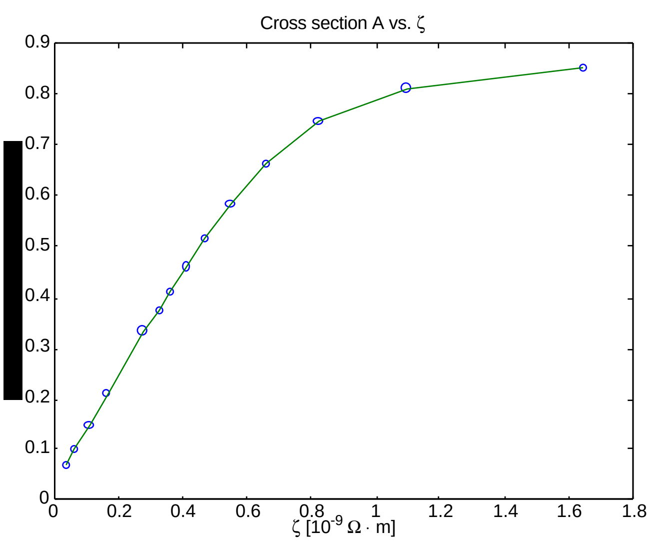

Fig. 6. Relationship between the parameter ζ and the area A_1 for optimal designs with fixed strand diameter.

Case 1: Fixed Strand Diameter

In this case, the winding is constructed of litz wire. The diameter of the individual strands is fixed, and we vary the number of strands to trade off ac and dc losses. This corresponds to the analysis in [12]. For any chosen number of strands, the overall winding area is determined, and the configuration must be selected to minimize proximity effect. For any given area, the optimum choice will be a configuration such as one of those shown in Figs. 2-4, regardless of whether the parameters are those chosen for Figs. 2-4. Our task is to chose which one; that is, to chose the area A_1.

To chose A_1 we start with total power loss (the sum of (3) and (2)), and set its derivative with respect to A_1 equal to zero. We find an implicit expression for A_1,

$$A_1 = \frac{16\sqrt{2}}{\pi}\left(\frac{\rho_c}{\omega F_p d}\right)\frac{1}{\sqrt{g(A_1)+g'(A_1)\cdot A_1}} \qquad (5)$$

where $g'()$ is the derivative of the function $g()$ with respect to its argument A_1. The function is determined by the core geometry only, not by the particular design parameters, which may be lumped in a constant

$$\zeta = \frac{\rho_c}{\omega F_p d} \qquad (6)$$

Equation (5) then becomes

$$A_1 = \frac{16\sqrt{2}}{\pi}\zeta\frac{1}{\sqrt{g(A_1)+g'(A_1)\cdot A_1}} \qquad (7)$$

which implicitly describes a relationship between the parameter ζ and the area A_1, plotted in Fig. 6.

Given the information in Fig. 6, one can find an optimal design for any set of parameters with this particular core by calculating ζ from (6), finding A_1 from Fig. 6, and then finding the optimal shape corresponding to that value of A_1 from Figs. 2-4. Thus, we have a simple method that extends the numerical optimization results to any design on the same core, without the need to repeat the computationally intensive optimization.

Case 2: Fixed Strand Number

This case applies to litz wire in which the number of strands is fixed, and we want to find the optimum strand diameter, or to single strand wire (which is simply a particular case of fixing the strand number—fixing it equal to one). In this case, the same approach leads to:

$$A_1 = \frac{8}{\pi}\left(\frac{\rho_c nN}{\omega^2 F_p^3}\right)^{1/3}\left(2g(A_1)+g'(A_1)\cdot A_1\right)^{-1/3}. \qquad (8)$$

Again, all the factors describing a particular design may be lumped into one parameter (named ξ for this case)

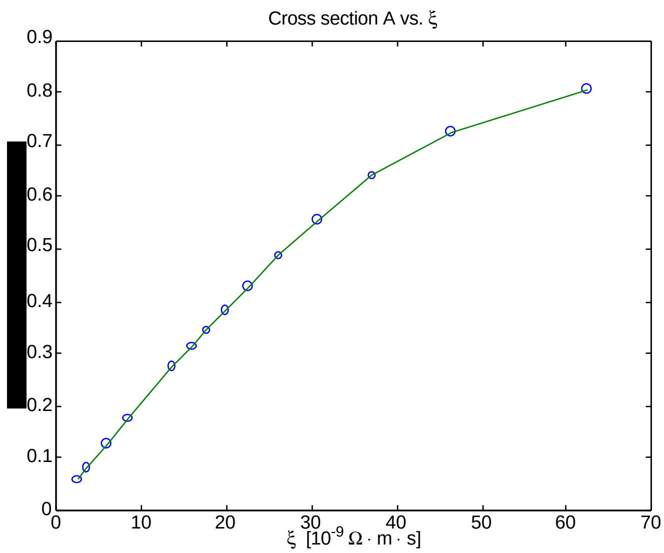

Fig. 7. Relationship between the parameter ξ and the area A_1 for optimal designs with number of strands fixed.

$$\xi = \left(\frac{\rho_c n N}{\omega^2 F_p^3} \right)^{1/3} \tag{9}$$

such that (8) becomes

$$A_1 = \frac{8}{\pi} \xi \left(2g(A_1) + g'(A_1) \cdot A_1 \right)^{-1/3} \tag{10}$$

which implicitly describes a relationship between ξ and A_1, plotted in Fig. 7 for the example geometry in Figs. 2-4. This plot provides the information needed to chose an optimal design for this core geometry, given a fixed number of strands, just as Fig. 6 provides the information needed to chose an optimal design given a fixed strand diameter.

IV. Discussion

Although the results in Section III provide the information needed to complete the design, additional ways of looking at the information lend more insight. In particular, a common way of discussing optimal winding designs is in terms of the optimal ac resistance factor $F_r = \frac{R_{ac}}{R_{dc}}$. The analysis in Section III can be used to derive expressions for optimal ac resistance factor [24]

$$F_r = 1 + \frac{g(A_1)}{g(A_1) + g'(A_1) \cdot A_1} \tag{11}$$

for fixed strand diameter (case 1) and

$$F_r = 1 + \frac{g(A_1)}{2 \cdot g(A_1) + g'(A_1) \cdot A_1} \tag{12}$$

for fixed strand number (case 2). These results can be related to previous results in the literature if we note that the standard one-dimensional analysis used for transformer windings corresponds to a value of $g()$ independent of the value of A_1, such that $g'() = 0$. These expressions ((11) and (12)) then reduce to $F_r = 2$ and $F_r = 1.5$. The latter is a familiar result [3-5, 22] for fixed strand number (usually for single-strand windings), and $F_r = 2$ is also the correct result for transformer windings with litz wire and a fixed strand diameter [23]. Thus, the new results represent a generalization of previous results.

The method developed here could be used in many ways. One use would be in magnetic component design, using standard cores. For a given core, the designer would perform a series of numerical optimizations to generate data like that

a)

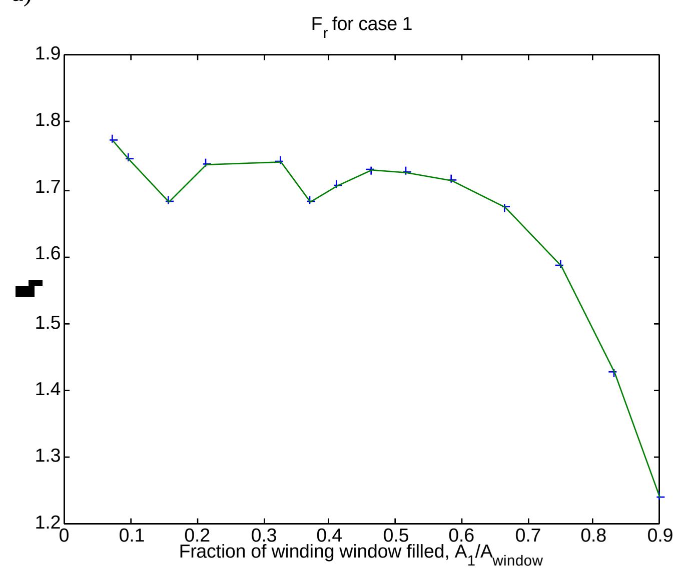

b)

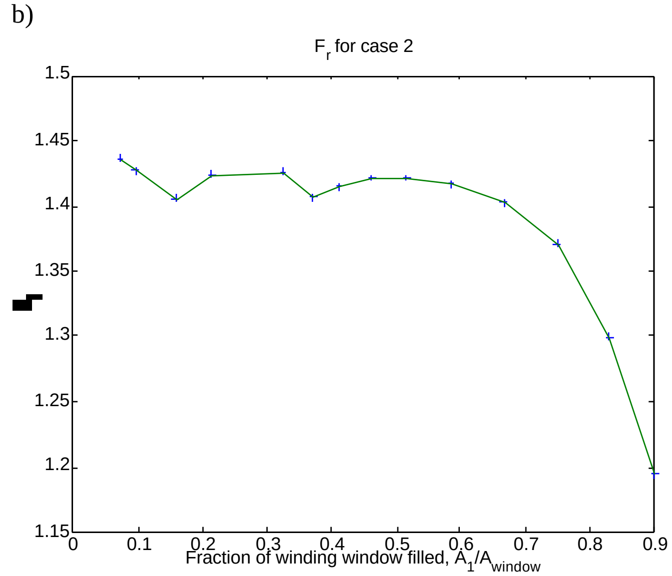

Fig. 8. Optimal ac resistance factor as a function of the fraction of the winding window filled, for two sets of constraints:
a) Case 1, fixed strand diameter, and
b) Case 2, fixed number of strands.

shown in Fig. 2-4. Then this data could be used to more quickly try a series of iterations for one design, or could used for different designs on the same core. A more attractive scenario would be for core manufacturers to publish the curves shown here for their core designs. Then any designer would be able to optimize designs without needing access to the specialized software developed in [12], and without needing to re-run computationally intensive numerical optimizations.

The litz-wire scenarios analyzed here are somewhat artificial, in that they require fixing either strand number or strand diameter. In practice, both variables may be adjusted, and considering both in an optimization may result in substantial loss and cost reduction, as demonstrated in [25] for transformer windings. Further work is needed to address this less-constrained optimization for inductors with optimized winding shapes.

The optimization in [12] upon which this work is based uses two-dimensional analysis. The approach developed here for generalizing the results would apply equally well to optimizations based on full three-dimensional or axisymmetric analysis. This makes three-dimensional analysis considerably more attractive, because even if it was not computationally efficient, once the analysis was done for a particular core shape, the approach here could allow it to be used in any design without the need for additional numerically intensive computation.

VI. Conclusion

Starting from a set of numerical optimizations for winding shape in a gapped inductor, we develop an analysis approach that allows finding optimal shapes for any design using the same core. Finding the optimal winding shape is then a matter of using simple calculations and graphical results. The results are shown to be consistent with previous results for transformer windings. The combination of a simple design approach and low losses with high ac current is promising for enabling wider application of soft-switching converter circuits that require high-ac-current inductors.

Appendix: Non-Sinusoidal Current Waveforms

In [23] it is shown that using Fourier analysis to represent a nonsinusoidal waveform and summing the losses for each harmonic is equivalent to using an effective frequency)

$$\omega_{eff} = \sqrt{\frac{\sum_{j=0}^{\infty} I_j^2 \omega_j^2}{\sum_{j=0}^{oo} I_j^2}} \tag{13}$$

as long as the skin depth for the highest important frequency is not small compared to the strand diameter.

Once the effective frequency of a pure ac waveform has been calculated, the effective frequency with a dc component can be calculated by a re-application of (13):

$$\omega_{eff} = \sqrt{\frac{I_{ac}^2 \omega_{eff,ac}^2}{I_{dc}^2 + I_{ac}^2}} \tag{14}$$

Finding Fourier coefficients and then summing the infinite series in (1) can be tedious. A shortcut, suggested but not fleshed out in [5], can be derived by noting that

$$\sum_{j=o}^{\infty} I_j^2 \omega_j^2 = \left[RMS\left\{ \frac{d}{dt} I(t) \right\} \right]^2 \tag{15}$$

so that

$$\omega_{eff} = \frac{RMS\left\{ \frac{d}{dt} I(t) \right\}}{I_{tot,rms}} \tag{16}$$

A symmetrical triangular current waveform with zero dc component results in an effective frequency of $1.103\omega_1$ where ω_1 is the fundamental frequency. Although the series in (1) does not converge for a square wave, and (4) is undefined, practical waveforms in inductors are never perfectly square. A square wave with finite-slope edges leads to a finite value of ω_{eff}, which can be found from (4) to be

$$\omega_{eff} = \frac{\omega_1}{\pi} \sqrt{\frac{6}{\Delta(3-4\Delta)}} \tag{17}$$

where Δ is the transition time as a fraction of the total period. For $\Delta = 0.5$ the waveform becomes triangular and (5) gives the same value of ω_{eff} as calculated above. This expression (5) is valid as long as there is not significant harmonic current for which the wire diameter is large compared to a skin depth. Based on the rule thumb that the highest important harmonic number is given by $N = 0.35\Delta$ [26], a rough check on this would be to calculate skin depth for a maximum frequency $\omega_{max} = \frac{0.35\omega_1}{\Delta}$, and compare this to the wire diameter.

REFERENCES

[1] A. M. Urling, A. V. Niemela, G. R. Skutt, and T. G. Wilson, "Characterizing High-Frequency Effects in Transformer Windings--A Guide to Several Significant Articles," in *APEC 89*, March 1989.

[2] P. L. Dowell, "Effects of Eddy Currents in Transformer Windings," *Proceedings of the IEE*, vol. 113, pp. 1387-1394, August 1966.

[3] J. Jongsma, "Minimum-Loss Transformer Windings for Ultrasonic Frequencies, Part 1: Background and Theory," *Phillips Electronics Applications Bulletin*, vol. E.A.B. 35, pp. 146-163, 1978.

[4] J. Jongsma, "Minimum-Loss Transformer Windings for Ultrasonic Frequencies, Part 2: Transformer winding design," *Phillips Electronics Applications Bulletin*, vol. E.A.B. 35, pp. 211-226, 1978.

[5] J. Jongsma, "High-Frequency Ferrite Power Transformer and Choke Design, Part 3: Transformer Winding Design," Phillips Electronic Components and Materials Technical Publication 207 1986.

[6] P. S. Venkatraman, "Winding Eddy Current Losses in Switch Mode Power Transformers Due to Rectangular Wave Currents," in *Proceedings of Powercon 11*, 1984.

[7] N. R. Coonrod, "Transformer Computer Design Aid for Higher Frequency Switching Power Supplies," in *IEEE Power Electronics Specialists Conference Record*, 1984.

[8] J. P. Vandelac and P. Ziogas, "A Novel Approach for Minimizing High Frequency Transformer Copper Losses," in *IEEE Power Electronics Specialists Conference Record*, 1987.

[9] J. A. Ferreira, "Improved analytical modeling of conductive losses in magnetic components.," *IEEE Transactions on Power Electronics*, vol. 9, pp. 127-31, January 1994.

[10] J. A. Ferreira, *Electromagnetic Modeling of Power Electronic Converters*: Kluwer Academic Publishers, 1989.

[11] R. Severns, "Additional losses in high frequency magnetics due to non ideal field distributions," in *APEC '92. Seventh Annual Applied Power Electronics Conference and Exposition*, Boston, MA, February 1992.

[12] J. Hu and C. R. Sullivan, "Optimization of Shapes for Round-Wire High-Frequency Gapped-Inductor Windings," in *IEEE Industry Applications Society 33rd Annual Meeting*, St. Louis, MO, 1998.

[13] D. T. N. Khai and M. H. Kuo, "Effects of Air Gaps on Winding Loss in High-Frequency Planar Magnetics," in *19th Annual Power Electronics Specialists Conf.*, April 1988.

[14] W. M. Chew and P. D. Evans, "High Frequency Inductor Design Concepts," in *22nd Annual Power Electronics Specialists Conf.*, June 1991.

[15] U. Kirchenberger, M. Marx, and D. Schroder, "A Contribution to the Design Optimization of Resonant Inductors in High Power Resonant Converters," in *1992 IEEE Industry Applications Society Annual Meeting*, October 1992.

[16] W. A. Roshen, R. L. Steigerwald, R. J. Charles, W. G. Earls, G. S. Claydon, and C. F. Saj, "High-efficiency, high-density MHz magnetic components for low profile converters," *IEEE Transaction on Industrial Applications*, vol. 31, July/August 1995.

[17] C. R. Sullivan and S. R. Sanders, "Design of Microfabricated Transformers and Inductors for High-Frequency Power Conversion," *IEEE Trans. on Power Electronics*, vol. 11, pp. 228-238, 1996.

[18] N. H. Kutkut, D. W. Novotny, D. M. Divan, and E. Yeow, "Analysis of Winding Losses in High Frequency Foil Wound Inductors," in *1995 IEEE Industry Applications Conference 30th IAS Annual Meeting*, October 1995.

[19] N. H. Kutkut and D. M. Divan, "Optimal air gap design in high frequency foil windings," in *IEEE Applied Power Electronic Conference*, Atlanta, February 1997.

[20] N. H. Kutkut, "A simple technique to evaluate winding losses including two dimensional edge effects," in *IEEE Applied Power Electronics Conference*, Atlanta, February 1997.

[21] J. Hu and C. R. Sullivan, "The quasi-distributed gap technique for planar inductors: Design guidelines," in *32nd IAS Annual Meeting*, New Orleans, October 1997.

[22] E. C. Snelling, *Soft Ferrites, Properties and Applications, second edition*: Butterworths, 1988.

[23] C. R. Sullivan, "Optimal Choice for Number of Strands in a Litz Wire Transformer Winding," *IEEE Transactions on Power Electronics*, vol. 14, pp. 283-291, 1999.

[24] J. Hu, *Design Techniques for High-Frequency Inductors—the Optimal Shape of the Winding and the Design of Quasi-Distributed Gaps*, M. S. Thesis, Thayer School of Engineering, Dartmouth College, 1998.

[25] C. R. Sullivan, "Cost-Constrained Selection of Number of Turns in a Litz-Wire Transformer Winding," in *IEEE Industry Applications Society 33rd Annual Meeting*, St. Louis, Missouri, 1998.

[26] J. G. Breslin and W. G. Hurley, "Derivation of optimum winding thickness for duty cycle modulated current waveshapes," in *Power Electronics Specialists Conference*, 1997.